Journal of Physiology (1993), **463**, *pp.* 141–155
With 7 figures
Printed in Great Britain

PERMEABILITY OF THE FETAL VILLOUS MICROVASCULATURE IN THE ISOLATED PERFUSED TERM HUMAN PLACENTA

BY BRYAN M. EATON, LOPA LEACH* AND J. ANTHONY FIRTH*

*From the Department of Obstetrics and Gynaecology, Charing Cross and Westminster Medical School, West London Hospital, London W6 7DQ and the *Department of Anatomy and Cell Biology, St Mary's Hospital Medical School, Imperial College of Science, Technology and Medicine, London W2 1PG*

(*Received 8 May 1992*)

SUMMARY

1. Capillary permeability–surface area (PS) products for the low molecular weight radioactive tracers, ^{22}Na, ^{51}Cr-EDTA (relative molecular mass 357) and ^{57}Co-cyanocobalamin (relative molecular mass 1353) were measured in the fetal circulation of isolated dually perfused lobules of normal term human placentae using the single circulation, multiple-tracer dilution technique.

2. In lobules perfused with M199 medium, containing dextran and 5 g l^{-1} bovine albumin, the extractions of all three tracers decreased as the flow was increased over the range of 2–8 ml min^{-1}, and PS products for ^{51}Cr-EDTA and ^{57}Co-cyanocobalamin, but not for ^{22}Na, reached constant values at flows above 0·1 ml min^{-1} g^{-1}.

3. Flow-independent PS products in the presence of albumin were $0{\cdot}025 \pm 0{\cdot}002$ ml min^{-1} g^{-1} (mean ± S.E.M., $n = 25$) for ^{57}Co-cyanocobalamin and $0{\cdot}057 \pm 0{\cdot}003$ ml min^{-1} g^{-1} ($n = 25$) for ^{51}Cr-EDTA. The ratio of PS values (^{51}Cr-EDTA/^{57}Co-cyanocobalamin) was 2·28, while the ratio of the corresponding free diffusion coefficients was 1·79, indicating substantial restriction to the diffusion of the ^{57}Co-cyanocobalamin.

4. In another series of lobules perfused in the absence of albumin, extraction values for all three test tracers were constant over the same flow range. Values at high flow rates were therefore about twice those measured in the presence of albumin, and PS products for all three tracers failed to reach diffusion-limited values.

6. Lobules perfused with and without albumin were fixed using a glutaraldehyde fixative containing 1% Alcian Blue dye. An ultrastructural examination of the endothelium showed no significant changes in cell or cleft morphology, or in the glycocalyx, in the absence of albumin which might account for the observed permeability change.

7. These data are the first physiological measurements specifically characterizing fetal microvascular permeability in the human placenta. The results suggest that permeability resembles that found in skeletal muscle and, as such, the endothelium presents a significant barrier to the diffusion of large solutes. The observed 'protein effect' indicates that albumin can interact with elements of the solute pathway to increase its restrictiveness.

MS 1353

INTRODUCTION

The human placenta at term provides a barrier regulating the transfer of materials between mother and fetus. In the areas of the terminal villi believed to be responsible for nutrient and gas exchange the placental interface consists of two major tissue layers: the syncytiotrophoblast, which is bathed on its microvillous surface with maternal blood flowing through the intervillous space, and the endothelium of the fetal villous circulation, separated from the syncytiotrophoblast by a composite basal lamina derived from both tissue layers. Placental physiologists have, until now, been largely concerned with the permeability of the whole interhaemal barrier and the individual contribution of the endothelium is unknown. An early electron microscopic study of the placental villous capillary endothelium indicated that it was a tight continuous endothelium resembling that found in brain more than that of muscle capillaries, and was characterized by the presence of *zonulae occludentes* blocking the intercellular spaces (Heinrich, Metz, Raviola & Forssmann, 1976). However, a recent study by Leach & Firth (1992) has shown that, in the terminal villi, the endothelial junctions consist of wide zones of uniform width interspersed with tight junctional regions which were found to be discontinuous along the axial length of the cleft.

These results suggest a structural similarity between human placental villous capillaries and continuous non-brain capillaries such as those of skeletal muscle (Simionescu, Simionescu & Palade, 1973) or heart (Ward, Bauman & Firth, 1988). As such, microvascular permeability in the human placenta appears to differ from physiological and morphological measurements obtained in the guinea-pig placenta, which is a commonly used animal model in placental transfer studies, and where substantial permeability to radioactive tracers (Eaton, Yudilevich, Bradbury & Bailey, 1977) and electron-dense macromolecules (Sibley, Bauman & Firth, 1982) has been demonstrated.

We report here the first measurements of fetal villous microvascular permeability–surface area (PS) products, obtained in isolated lobules of normal term human placenta, using a well-established, multiple-tracer dilution technique (Martín de Julían & Yudilevich, 1964; see Bassingthwaighte & Goresky, 1984 and Crone & Levitt, 1984 for reviews). The data suggest that the capillaries exhibit permeability characteristics similar to those of skeletal muscle and, as such, probably contribute substantially to the restricted transplacental movement of high molecular weight substances. A preliminary account of some of these studies has been presented in abstract form (Eaton, Leach & Firth, 1992).

METHODS

Placental preparation

Normal term human placentae were obtained at elective Caesarian section. Perfusion of the fetal circulation in a selected, intact lobule was started, within 5 min of delivery of the placenta, by inserting a cannula into the fetal chorionic artery supplying the lobule. The fetal venous drainage was collected from a cannula introduced into the corresponding chorionic vein via the umbilical vein. The placenta was then inverted (maternal surface uppermost) and the perfused area was isolated from the rest of the placenta by clamping the lobule inside an annular Perspex chamber (6·5 cm diameter). The maternal circulation was established by inserting five cannulae, fed from a

distribution head, through the basal plate of the lobule into the intervillous space. Both the fetal and maternal circulations of the selected lobule were perfused in open circuit. Preparations were perfused for an initial stabilizing period of 20 min. This has been shown to restore normal placental function and structure following the ischaemia and hypoxia associated with delivery of the placenta (Bloxham & Bullen, 1986; Leach & Firth, 1992). During this period the fetal flow was

TABLE 1. Relative molecular mass, Stokes–Einstein radius and free diffusion coefficients in water at 37 °C (D_{37}) for the tracer molecules used in this study (data are taken from Sweiry & Mann, 1991)

Tracer	Relative molecular mass	Molecular radius (nm)	D_{37} ($cm^2\ s^{-1} \times 10^{-5}$)
^{22}Na	22	0·23	1·80
^{51}Cr-EDTA	357	0·47	0·70
^{57}Co-cyanocobalamin	1353	0·84	0·39
^{125}I-albumin	~ 66000	3·61	0·093

maintained at 6 ml min^{-1} and the maternal flow was 20 ml min^{-1}. Perfusion pressures were monitored proximal to the site of insertion of the arterial cannulae. Initial perfusion pressures on the fetal side ranged between 20 and 80 mmHg while the maternal side perfusion pressure was always below 20 mmHg. The procedures and perfusion apparatus have previously been described in detail (Contractor, Eaton, Firth & Bauman, 1984).

Experiments were performed on ten isolated, dually perfused lobules of normal term human placenta. Six lobules were perfused in the presence of 5 g l^{-1} bovine serum albumin in the perfusate and four in the absence of albumin. The weights of the perfused lobules in the two groups were 38·0 ± 4·2 g (mean ± S.E.M., $n = 6$) and 45·2 ± 3·2 g ($n = 4$) respectively, and were not statistically different (t test).

Perfusates

The perfusate for both the maternal and fetal circuits was M199 tissue culture medium to which was added 2·2 g l^{-1} sodium bicarbonate, 100 μM adenosine to ensure maximal vasodilatation of the fetal capillary bed (Wheeler & Yudilevich, 1988; Reviriego Alonso, Ibañez & Marín, 1990), 2 mg l^{-1} cyanocobalamin (vitamin B_{12}) to saturate carrier-mediated uptake mechanisms for this vitamin (Mann, Smaje & Yudilevich, 1979), and 8 g l^{-1} of dextran (~ 20000 relative molecular mass) as the oncotic agent. This perfusate had a mean osmolarity of 292 ± 3 (mean ± S.E.M., $n = 14$) mosmol l^{-1}. In some experiments perfusates also contained 5 g l^{-1} bovine albumin. The perfusion media and all chemicals were obtained from Sigma Chemical Co. (Poole, Dorset). Perfusates were oxygenated with 95% O_2, 5% CO_2.

Radioactive tracer molecules

^{22}Na and ^{57}Co-cyanocobalamin were purchased from Amersham International, PLC, (Amersham, Bucks) and ^{51}Cr-EDTA was obtained from NEN (Du Pont UK Ltd, Stevenage, Herts). The intravascular reference tracer, ^{125}I-bovine albumin, was prepared from bovine serum albumin (Sigma) and carrier-free ^{125}I (Amersham) using the iodogen procedure (Fraker & Speck, 1978). The iodinated protein was purified on a Sephadex G25 (Pharmacia Ltd, Milton Keynes) column, to remove free iodine and low molecular weight breakdown products, immediately prior to use. Hence, < 2% of ^{125}I-albumin activity was found to be non-precipitable in the presence of 10% trichloroacetic acid. The physical characteristics of the tracers used in this study are listed in Table 1.

Single-passage, multiple-tracer experiment

In most perfusions eight successive multiple-tracer dilution experiments were performed in each lobule, with duplicate determinations being made at four fetal flow rates (2, 4, 6 and 8 ml min^{-1}), in random order. A 100 μl bolus containing the four radioactive tracers was rapidly injected (~ 2 s) into the fetal arterial inflow cannula and, after a predetermined delay (dependent on the perfusion flow), thirty samples, each containing two drops of the fetal venous outflow, were subsequently collected from the chorionic vein. At the end of the collection the fetal venous outflow was pooled for a further 3 min period. This provided a measurement of the venous flow rate and

aliquots of this sample could be removed for counting in order to obtain total tracer recovery data over a period of 3·5–5 min following the bolus injection. Only data from experiments where the measured fetal inflow and outflow rates were similar were used. Background samples, single isotope standards, sequential run samples and 3 min sample aliquots, as well as aliquots of the isotope mixture, were counted in a 4-channel scintillation counter (LKB 1282, Pharmacia) using predetermined windows which minimized cross-channel overlap without substantially reducing counting efficiency.

Data analysis

Data were analysed on a microcomputer, using a BASIC program, based on the procedure described by Martín de Julían & Yudilevich (1964). Sample counts were corrected for background and cross-channel contamination and the activities of the four tracers in the successive venous samples were expressed as percentages of the injected dose. Test tracer extractions (E) were calculated from the individual sample data using the relationship:

$$E = 1 - c_t/C_t,$$

where c_t is the test tracer concentration and C_t is the concentration of the ^{125}I-albumin. Extraction values for the test tracers were plotted against the accumulated reference tracer (albumin) recovery as a means of weighting the samples. It was found that extraction curves generally exhibited an initial maximal plateau area comprising values from four to eleven samples. Hence, values within these plateau regions were averaged to produce the mean extraction values.

Extraction values were used to calculate permeability–surface area (PS) products using the relationship developed by Renkin (1959) and Crone (1963):

$$\mathrm{PS} = -F \ln (1-E)\ \mathrm{ml\ min^{-1}\ g^{-1}},$$

where E is the tracer extraction and F is the fetal perfusion flow per gram of tissue. Data were kept in this form to facilitate comparisons with other tissues. Detailed capillary surface area data (in units of $\mathrm{cm^2\ cm^{-3}}$) are not available for the human placenta, precluding calculation of permeability coefficients.

Ultrastructural studies

At the end of the tracer study (usually about 60 min) the perfusate on the fetal side was changed to a mixture of 2% glutaraldehyde and 2% freshly prepared paraformaldehyde in 0·06 M sodium cacodylate–HCl buffer, pH 7·3. The tissue was perfusion fixed for 30 min and the fixed area was excised, blotted dry and weighed. It was subsequently cut into 1 $\mathrm{mm^3}$ cubes and immersion fixed for a further 60 min before being transferred to a cacodylate buffer containing 0·5 M sucrose. Tissue pieces were post-fixed for 1 h in 1% osmium tetroxide, dehydrated and embedded in Araldite (Taab Laboratory Equipment Ltd, Aldermaston, Berks). Semi-thin sections were stained with Toluidine Blue to locate terminal villous capillaries. Suitable blocks were sectioned (70 nm thick) and stained with uranyl acetate and lead citrate. Twenty capillaries from each perfused lobule were viewed under a Jeol 100CX electron microscope and checked for ultrastructural signs of ischaemic degeneration. Data obtained from placentae showing morphological damage were discarded.

Membrane imaging and goniometric analyses

Two placentae from the albumin-free group and two from the albumin group were fixed and prepared for electron microscopy as described above, but were post-fixed in 1% osmium tetroxide containing 1·5% potassium ferrocyanide to mordant the tissue. This improves membrane imaging, so facilitating measurements of membrane spacing and also reveals linkers in the paracellular clefts (Leach & Firth, 1992). Ultra-thin sections of five microvessels from each of the four placentae were obtained as described above. Twenty paracellular clefts were observed at a magnification of × 160000. The thin sections were rotated so that junctional zones of paracellular clefts were aligned along the tilt axis of the goniometer stage. The junctions were then photographed every 5 deg over a range of tilt angles which bracketed the point of maximal membrane clarity. The distances between the two membranes at the tight junctional regions and adjoining wide zones were measured on prints (magnification × 256000) using an eyepiece graticule (Leach & Firth, 1992).

Alcian Blue staining of the glycocalyx

In two experiments in which the lobules were perfused with either albumin-containing or albumin-free perfusates the fixative contained 1% Alcian Blue 8GX (Gurr, BDH Chemicals, Poole, Dorset). This electron-dense dye, which binds to anionic sites has been used in ultrastructural

studies to visualize the glycocalyx (Montesano, Mossaz, Ryser, Orci & Vassalli, 1984). Previous studies using Ruthenium Red as an alternative label to visualize the glycocalyx (Baldwin & Winlove, 1984) showed that this larger molecular weight marker was subject to steric hindrance and was not suitable for labelling the glycocalyx in the presence of serum proteins. In experiments using albumin-containing perfusates the fetal vasculature was flushed through with an albumin-free perfusate for 2 min prior to fixation to remove intravascular albumin. Tissue was prepared for electron microscopy as described above and the Alcian Blue-stained microvessels (ten from each experiment) were photographed at $\times 160000$ magnification to show the luminal glycocalyx and the intercellular cleft region.

Statistical analysis

All data are presented as means $\pm$ S.E.M. and significance was determined using an unpaired t test.

RESULTS

Figure 1*A* shows typical outflow dilution profiles obtained from the chorionic venous cannula following the injection of a bolus containing the four radioactive tracers into the chorionic arterial cannula supplying the perfused lobule. The experiment was performed at a flow of 6 ml min^{-1} in the presence of 5 g l^{-1} albumin. The activities of the four tracers in the successive outflow samples are plotted as percentages of the quantities injected (to normalize the data) against the collection time in seconds. The dilution profiles for the three permeant tracers, ^{57}Co-cyanocobalamin, ^{51}Cr-EDTA and ^{22}Na all initially fall below that of the intravascular reference tracer, ^{125}I-albumin. This indicates that, during the single passage through the fetal villous circulation in the perfused lobule, the three test tracers left the intravascular space marked by the albumin and passed out into the interstitium. The total recoveries of the four tracers over the 3·75 min collection period were: ^{125}I-albumin, 96·3%, ^{57}Co-cyanocobalamin, 95·0%, ^{51}Cr-EDTA, 90·2% and ^{22}Na, 84·7%. The combined data from all dilution curves in ten experiments performed in the presence or absence of albumin gave an ^{125}I-albumin recovery of $101·9 \pm 1·7$% ($n = 67$).

The fractional extractions of the permeant tracers were quantified in the successive venous samples using the relationship described in the Methods, and the values are plotted in Fig. 1*B* against the accumulated reference tracer recovery. This is a means of weighting the individual samples which prevents those with low activities (associated with large counting errors) being given an equal weighting to samples containing substantial numbers of counts. The points in the initial plateau region of the extraction curves were averaged to calculate the mean extraction values. Extraction curves for ^{57}Co-cyanocobalamin and ^{51}Cr-EDTA always had substantial initial plateau regions and did not lend themselves well to the zero time extrapolation procedure described by Martín de Julían & Yudilevich (1964). The ^{22}Na curves frequently exhibited an obvious initial plateau region, but occasionally backflux occurred quite rapidly (Fig. 1*B*). A statistical analysis (paired t test) of maximal extraction values averaged from the first three to five samples and the zero-time extraction values (E_0) showed that they were not significantly different. Hence plateau values were used in all subsequent analyses.

Figure 2 is a plot of the individual extraction values obtained in the presence of albumin-containing perfusates. Each point represents an individual measurement, and the extraction values for the three permeant tracers, calculated as described above, are plotted against the flow (in ml min^{-1} g^{-1}). Also plotted is the calculated

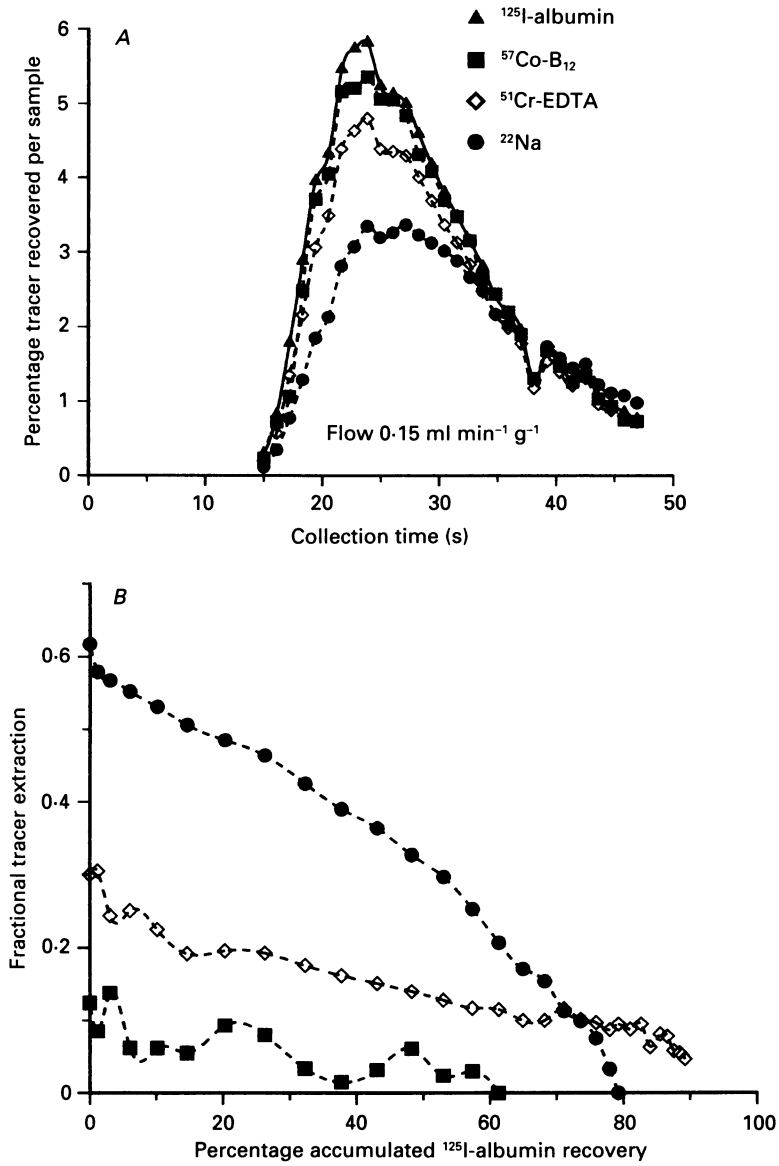

Fig. 1. Analysis of single-circulation, multiple-tracer dilution curves. *A*, venous outflow concentration profiles for the four tracers are plotted against the collection time. Concentrations have been normalized with respect to the injected quantities of the tracers. *B*, fractional extraction values for the three test tracers in the consecutive samples, calculated relative to the ^{125}I-albumin concentrations, are plotted against the accumulated area under the ^{125}I-albumin dilution curve as a means of weighting the individual extraction values.

linear regression line for each set of data. It can be seen that extraction values decrease with increasing molecular weight and that, within each band, there is a flow-dependent fall in extraction over the range studied. The negative slopes of the regression lines plotted for each data set are statistically significant for all three

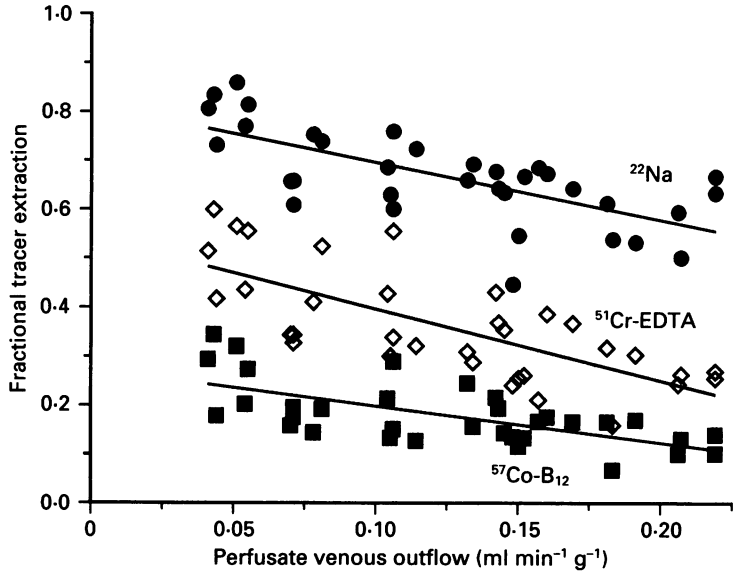

Fig. 2. Effect of perfusion flow on capillary solute extraction. Combined extraction data for the three test solutes, obtained in the presence of albumin, are plotted against the perfusion flow. Each point represents an individual measurement. The regression lines plotted for each tracer have correlation coefficients of $-0{\cdot}642$ for ^{22}Na, $-0{\cdot}722$ for ^{51}Cr-EDTA and $-0{\cdot}686$ for ^{57}Co-cyanocobalamin (B_{12}); $P < 0{\cdot}001$ in all cases.

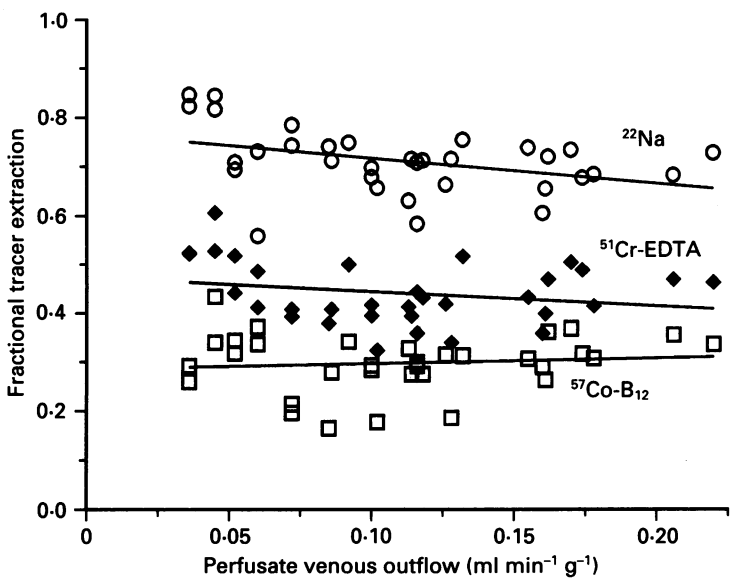

Fig. 3. Effect of perfusion flow on capillary solute extraction in the absence of albumin. Each point represents an individual measurement of extraction. The slopes of the calculated regression lines are not statistically significantly different from zero.

tracers ($P < 0{\cdot}001$). In contrast Fig. 3 illustrates a similar plot from four experiments in the absence of albumin. The calculated slopes of the regression lines for the combined data were not statistically different from zero in all cases.

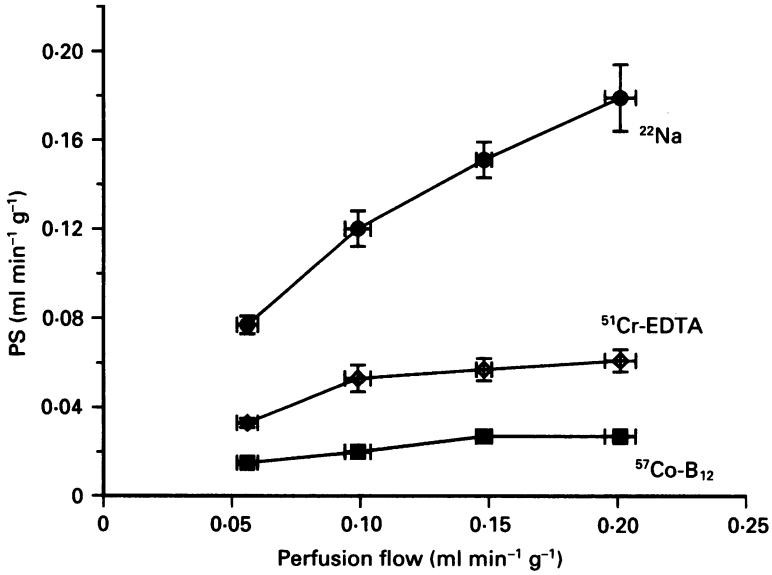

Fig. 4. Effects of flow on permeability surface area (PS) products. PS values for ^{22}Na, ^{51}Cr-EDTA and ^{57}Co-cyanocobalamin (B_{12}), obtained in the presence of 5 g l^{-1} albumin in the perfusate, were grouped into one of four flow ranges (see text). Data are plotted as means ± S.E.M. of 5–11 values, with error bars for both PS and flow determinations.

TABLE 2. Effect of flow on extraction and PS values for ^{51}Cr-EDTA and ^{57}Co-cyanocobalamin obtained in the presence and absence of albumin

	Flow (ml min^{-1} g^{-1})			
	0·025–0·075	0·075–0·125	0·125–0·175	0·175–0·225
	With albumin			
E_{EDTA}	0·456 ± 0·035 (9)	0·411 ± 0·037 (7)	0·316 ± 0·021 (11)	0·259 ± 0·019 (7)
$E_{B_{12}}$	0·238 ± 0·023 (9)	0·180 ± 0·022 (7)	0·169 ± 0·021 (11)	0·126 ± 0·014 (7)
PS_{EDTA}	0·033 ± 0·002 (9)	0·053 ± 0·006 (7)	0·057 ± 0·005 (11)	0·061 ± 0·005 (7)
$PS_{B_{12}}$	0·015 ± 0·001 (9)	0·020 ± 0·003 (7)	0·027 ± 0·002 (11)	0·027 ± 0·003 (7)
	Albumin-free			
E_{EDTA}	0·484 ± 0·022 (10)	0·406 ± 0·014 (11)	0·437 ± 0·021 (9)	0·450 ± 0·017 (3)
$E_{B_{12}}$	0·317 ± 0·023 (10)	0·280 ± 0·018 (11)	0·303 ± 0·018 (9)	0·334 ± 0·014 (3)
PS_{EDTA}	0·034 ± 0·002 (10)	0·054 ± 0·003 (11)	0·085 ± 0·007 (9)	0·121 ± 0·013 (3)
$PS_{B_{12}}$	0·020 ± 0·002 (10)	0·035 ± 0·003 (11)	0·056 ± 0·005 (9)	0·082 ± 0·008 (3)

Values are given as means ± S.E.M., with the number of experimental observations (n) in parentheses. PS values are in ml min^{-1} g^{-1}.

The ^{51}Cr-EDTA and ^{57}Co-cyanocobalamin extraction data from these two series of experiments are presented in Table 2, grouped over four equal flow ranges (0·025–0·075, 0·075–0·125, 0·125–0·175 and 0·175–0·225 ml min^{-1} g^{-1}). It can be seen that even at low flows the extraction values for both tracers are higher in the absence of albumin. Moreover, in the absence of protein there is very little change in the

extraction values for ^{51}Cr-EDTA or ^{57}Co-cyanocobalamin as the flow increased. Hence, at the highest flows, the extraction values for ^{57}Co-cyanocobalamin and ^{51}Cr-EDTA, in the absence of albumin, are about twice those obtained in the presence of albumin.

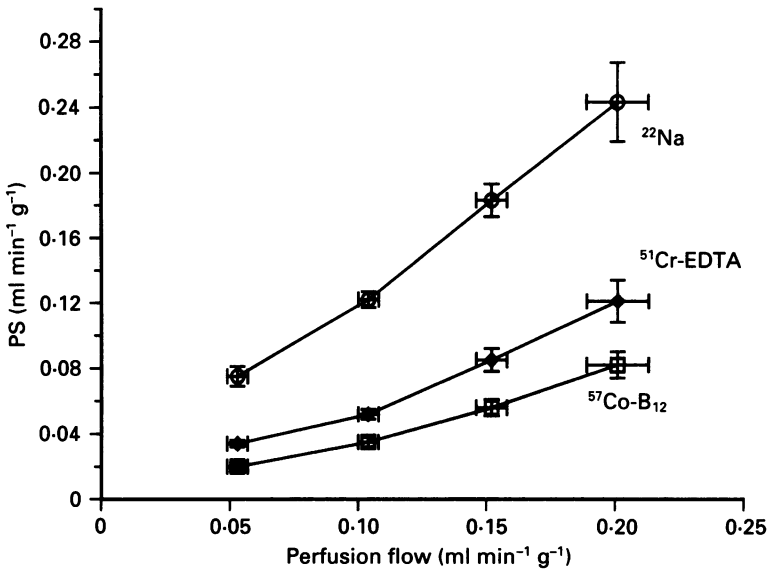

Fig. 5. Effects of flow on permeability surface area (PS) products measured in the absence of albumin in the perfusate. Values were treated as described in Fig. 4. and similarly plotted.

The extraction data obtained in the presence or absence of albumin were fitted to the Renkin–Crone equation to calculate permeability–surface area (PS) products. PS values for all three tracers were grouped within the same flow ranges and data obtained in the presence of albumin are plotted in Fig. 4 as mean PS against mean flow rates. Standard error bars for both variables are also plotted. It can be seen that at the higher flows studied the PS values for ^{57}Co-cyanocobalamin and ^{51}Cr-EDTA became independent of flow (see Table 2) and hence provide an estimate of diffusion-limited permeability. PS data from the three highest flow ranges were therefore combined. This resulted in a PS value for ^{57}Co-cyanocobalamin of $0{\cdot}025 \pm 0{\cdot}002$ ml min^{-1} g^{-1} ($n = 25$) and for ^{51}Cr-EDTA of $0{\cdot}057 \pm 0{\cdot}003$ ml min^{-1} g^{-1} ($n = 25$). In contrast, despite the flow-dependent reduction in extraction values for ^{22}Na (Fig. 2) the PS curve continued to rise even at the highest flows tested and therefore all PS estimates for ^{22}Na are flow dependent.

In the absence of albumin, PS curves for all three tracers when plotted similarly (Fig. 5) continued to rise sharply with increasing flow and diffusion-limited PS values, independent of flow, were not reached within the physiological range used (Table 2). Flows higher than 8 ml min^{-1} could not be used because they resulted in extensive ultrastructural damage (data not shown).

Endothelial cells from placentae perfused for 90 min with either albumin-containing or albumin-free perfusates showed a similar cleft and cell morphology to that of placentae perfused for only the 20 min equilibration period (Leach & Firth, 1992). Placental microvessels were seen to possess one to four paracellular clefts per cross-sectional profile. The fine structure of the paracellular clefts (Fig. 6) revealed

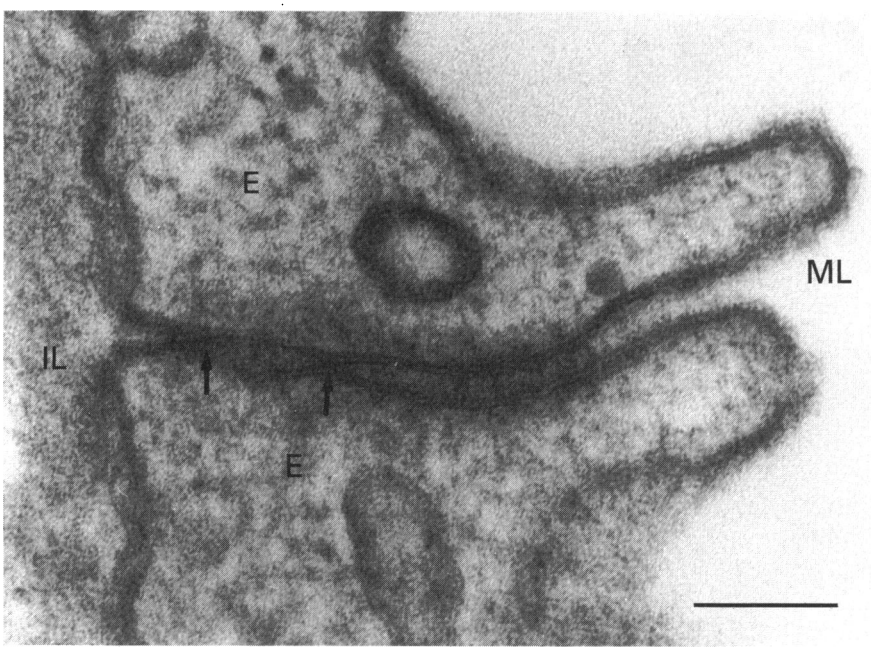

Fig. 6. Micrograph showing organization of the paracellular cleft of fetal microvascular endothelium (E) from a placenta perfused in the presence of albumin for 90 min, and post-fixed in 1% osmium tetroxide containing 1·5% potassium ferrocyanide to enhance membrane imaging. The paracellular cleft can be seen to contain two tight junctional regions (↑) where the plasmalemmal membrane leaflets of adjoining endothelial cells appear in close apposition. The tight junctional regions are interspersed with wide zones bridged at intervals with linkers. IL, interstitial layer; ML, microvessel lumen. Tilt angle = −20 deg. Bar = 0·1 μm.

one to four tight junctional regions per cleft. At some angle of tilt, the two outer leaflets of the apposed membranes were seen to possess a separation of $3{\cdot}4 \pm 0{\cdot}4$ nm ($n = 5$) in the presence of albumin, which was not significantly different from that obtained in the absence of albumin ($4{\cdot}1 \pm 0{\cdot}2$ nm, $n = 10$, $P > 0{\cdot}7$). Corresponding measurements for the wide regions of the clefts were $14{\cdot}9 \pm 0{\cdot}3$ nm ($n = 45$) and $15{\cdot}6 \pm 0{\cdot}3$ nm ($n = 48$, $P > 0{\cdot}1$) respectively. The wide regions appear to be bridged at intervals with electron-dense 'linkers' under these experimental conditions.

In the experiments where 1% Alcian Blue was included in the fixative the glycocalyx was seen as a wide dense band on the luminal surface of the cell, which extended into the paracellular cleft. The width and density of the glycocalyx showed variation between capillaries and also within a single capillary in placentae perfused both in the presence (Fig. 7*A*) and in the absence (Fig. 7*B*) of albumin.

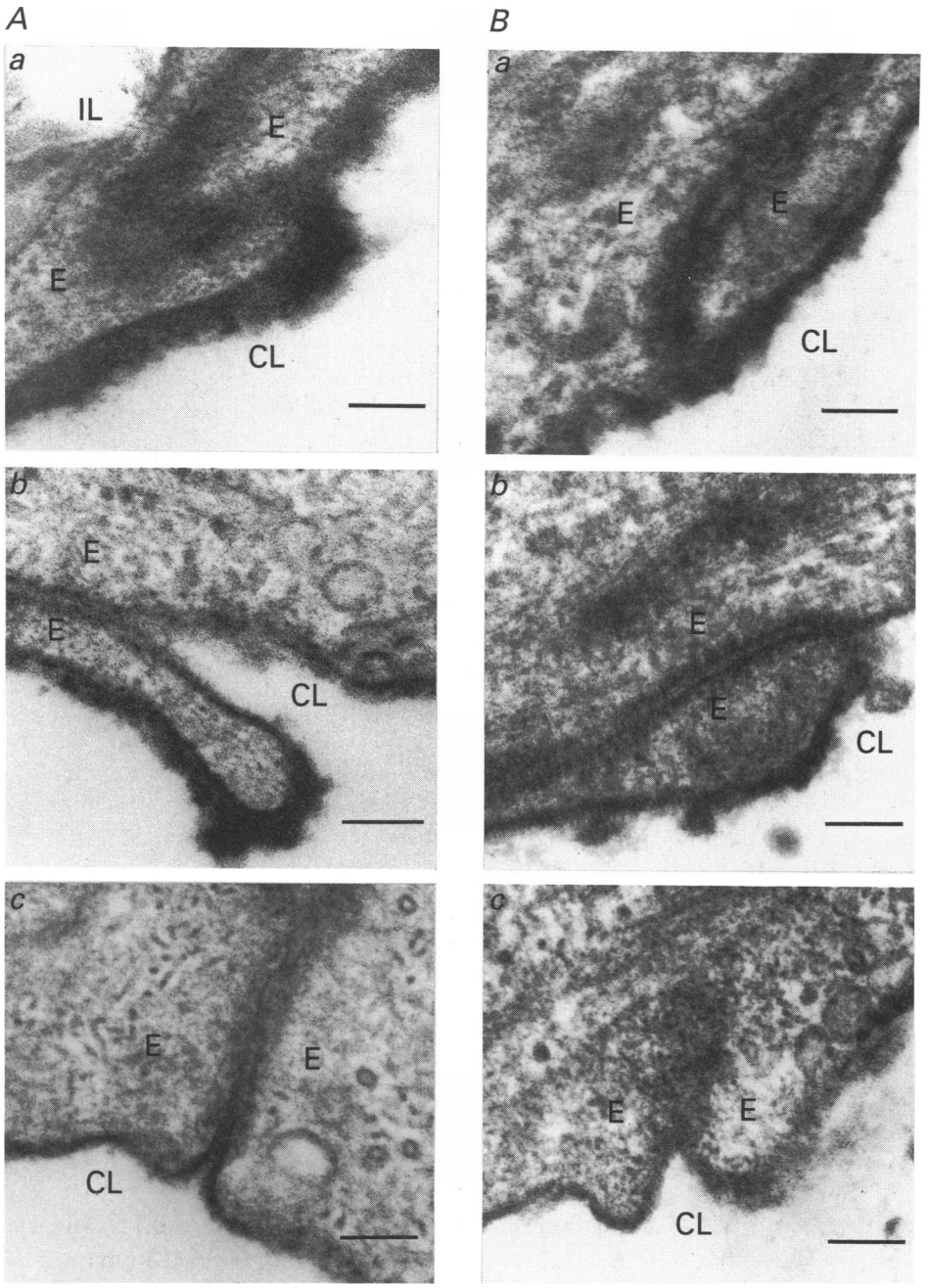

Fig. 7. Electron micrographs of fetal microvascular endothelium (E) of term human placentae showing the luminal surfaces at the paracellular cleft regions. At the end of the tracer experiments the placentae were perfused with fixative containing 1% Alcian Blue to stain the glycocalyx layer. Panel *A* shows the variation in the width and density of the glycocalyx observed in capillaries perfused in the presence of albumin. Panel *B* shows a similar variation in capillaries perfused with albumin-free solutions. IL, interstitial layer; CL, capillary lumen. Bar = 0·1 μm.

DISCUSSION

This study provides the first physiological data specifically describing the permeability characteristics of the fetal microvascular endothelium in the term human placenta to low molecular weight molecules. In addition, this is the first time, to our knowledge, that the 'protein effect' on permeability has been demonstrated in a perfused human vascular network. The well-established, multiple-tracer dilution technique used in this study provides estimates of permeability–surface area products which can be compared with those obtained by similar methods in a range of other tissue. Paaske & Sejrsen (1989) have recently reviewed the techniques used to measure the permeability of continuous capillaries and a critical discussion of the indicator-dilution method can be found therein. A comparison of the PS values obtained using this technique, under conditions which exclude a flow-dependent contribution to the measurement, indicate that placental capillaries most closely resemble skeletal muscle capillaries in their permeability characteristics (Trap-Jensen & Lassen, 1970; Paaske, 1977), and are more permeable than brain capillaries (Yudilevich & de Rosa, 1971) but far less permeable than heart capillaries (Mann, 1981) or the fenestrated capillaries in pancreas (Sweiry & Mann, 1991) or salivary gland (Mann *et al.* 1979).

The vascular network in the terminal villi consists of two separate capillary plexuses each main artery being accompanied by a paravascular and a superficial capillary network. While an early electron microscopic study of terminal villous capillaries suggested the presence of tight junctions between endothelial cells similar to those seen in the brain (Heinrich *et al.* 1976), this has not been confirmed by a recent study of intercellular clefts in these vessels (Leach & Firth, 1992). These authors found that intercellular junctions had a mean width of 15·6 nm, and serial sectioning revealed that each cleft usually contained one to four tight regions. Each tight junction apposition was found, by goniometric tilting, to have a separation of 4·1 nm between the outer leaflets of the adjoining plasma membranes. Furthermore, these lines of cell-to-cell contact were not continuous throughout the axial length of the capillaries. They concluded that the placental capillaries most resembled non-CNS continuous capillaries. Although in the present study we sampled a smaller number of microvessels, we observed a similar ultrastructural organization of the paracellular clefts in placentae perfused for 90 min (Fig. 6) as in the previous study, where lobules were perfused for only 20 min (Leach & Firth, 1992). These results thus provide ultrastructural support for the physiological measurements of permeability presented here.

The relationship between microvascular permeability and ultrastructure has been recently reviewed (Clough, 1991). The inadequacies of an ultrastructural correlate for the cylindrical pore theory developed by Pappenheimer, Renkin & Borrero (1951) led to the fibre matrix theory (Curry & Michel, 1980; see reviews by Curry, 1986 and Michel, 1988). In this model the hydraulic resistance of the pathway is defined by both the dimensions of the pores and the modulating effect on solute entry of the fibre matrix on the cell surface (glycocalyx) and in the junctional cleft region. The role of protein in modulating permeability was systematically studied in Michel's laboratory (Levick & Michel, 1973; Mason, Curry & Michel, 1977). They showed that

albumin concentrations as low as 1 mg ml^{-1} will prevent increases in hydraulic conductivity in Ringer solution-perfused frog single mesenteric capillaries. This effect of serum proteins on maintaining 'normal' permeability has been reported in many other systems, e.g. rabbit heart (Mann, 1981), rat lung (Schneeberger & Hamelin, 1984) and rat muscle (Haraldsson & Rippe, 1985). Of the serum proteins involved (including immunoglobulin G and orosmomucoid), albumin appears quantitatively the most important (see Michel, 1988 for review). Schneeberger & Hamelin (1984) demonstrated albumin in the wide regions of the cleft but found it excluded from the tight regions. Hence removal of albumin may increase permeability of the wide regions without affecting the narrow regions.

In the present study the largest test tracer, ^{57}Co-cyanocobalamin, has a molecular radius of 0·84 nm which is nearly one-fifth of the minimum gap width in the tight regions of the endothelial gap junctions (Leach & Firth, 1992). If the diffusion of the permeant tracers ^{57}Co-cyanocobalamin and ^{51}Cr-EDTA was through a limited number of large pores, the ratio of their mean PS products (2·28) should equal the ratio of their free diffusion coefficients in water (1·79). The observed inequality is itself indicative of restricted diffusion (see Mann *et al.* 1979 for discussion) in the presence of albumin. The increased extractions at high flow in the absence of albumin suggest increased access to these limiting areas. The observation that, even in the tight regions of the intercellular junctions, the mean gap diameter is nearly 18 times larger than the diameter of ^{22}Na (Leach & Firth, 1992; Table 1) accounts for the increasing PS values for this tracer found both in the presence and absence of albumin.

Clough (1991) reviews evidence for the link between albumin and the glycocalyx in frog mesenteric capillaries by showing that re-perfusion with albumin-containing solutions causes 'lifting' of the glycocalyx (previously labelled with ferritin in the absence of protein), i.e. albumin increased the diffusional pathway for solutes to traverse. In our perfusion system the variation in the width of the glycocalyx observed for placentae perfused for about 90 min with albumin-containing (Fig. 7*A*) or with albumin-free (Fig. 7*B*) perfusates means that we cannot assert that albumin either alters the thickness of, or causes any observable structural changes to, the luminal glycocalyx. It is apparent, however, that the permeability effect in the absence of albumin cannot be correlated with any observable changes in endothelial morphology or tissue damage.

It is concluded that the permeability of the fetal capillaries in the term human placenta resembles that of skeletal muscle both physiologically and ultrastructurally and that solute movement may be modulated by the presence of albumin in the perfusate. The human placenta lacks a lymph drainage system and in other species this has been associated with the fetal endothelium providing most of the resistance to the transplacental transfer of large molecules (Thornburg & Faber, 1976; Boyd, Canning, Stacey, Ward & Weedon, 1983). *In vivo* transfer data in human placenta (Bain, Copas, Landon & Stacey, 1988; Bain, Copas, Taylor, Landon & Stacey, 1990) would lend support to the conclusion that the endothelium exerts a major regulatory role in transplacental transfer.

This work was funded by the Wellcome Trust (J.A.F.) and the University of London, Central Research Fund (B.M.E.). B.M.E. is grateful to Professor David Yudilevich for stimulating interests in both microvascular permeability and placenta. We are also grateful to Mr B. Crook for technical assistance, Dr J. Sweiry (King's College, London) for help with counting procedures, and to the midwives in the Alex Bourne 1 Labour Ward at St Mary's Hospital for supplying placentae.

REFERENCES

BAIN, M. D., COPAS, D. K., LANDON, M. J. & STACEY, T. E. (1988). *In vivo* permeability of the human placenta to inulin and mannitol. *Journal of Physiology* **399**, 313–319.

BAIN, M. D., COPAS, D. K., TAYLOR, A., LANDON, M. J. & STACEY, T. E. (1990). Permeability of the human placenta *in vivo* to four non-metabolized hydrophilic molecules. *Journal of Physiology* **431**, 505–513.

BALDWIN, A. L. & WINLOVE, C. P. (1984). Effects of perfusate composition on binding of Ruthenium red and gold colloid to glycocalyx of rabbit aortic endothelium. *Journal of Histochemistry and Cytochemistry* **32**, 259–266.

BASSINGTHWAIGHTE, J. B. & GORESKY, C. A. (1984). Modeling in the analysis of solute and water exchange in the microvasculature. In *Handbook of Physiology*, section 2, *The Cardiovascular System*, vol. IV, part 1 *Microcirculation*, ed. RENKIN, E. M. & MICHEL, C. C., pp. 549–626. American Physiological Society, Bethesda, MD, USA.

BLOXAM, D. L. & BULLEN, B. E. (1986). Condition and performance of the perfused human placental cotyledon. *American Journal of Obstetrics and Gynecology* **155**, 382–388.

BOYD, R. D. H., CANNING, J. F., STACEY, T. E., WARD, R. T. H. & WEEDON, A. P. (1983). Volumes of distribution of sodium and albumin in the sheep placenta. *Journal of Physiology* **336**, 13–26.

CLOUGH, G. (1991). Relationship between microvascular permeability and ultrastructure. *Progress in Biophysical and Molecular Biology* **55**, 47–69.

CONTRACTOR, S. F., EATON, B. M., FIRTH, J. A. & BAUMAN, K. F. (1984). A comparison of the effects of different perfusion regimes on the structure of the isolated human placental lobule. *Cell and Tissue Research* **237**, 609–617.

CRONE, C. (1963). The permeabilities of capillaries in various organs as determined by the use of the 'indicator diffusion method'. *Acta Physiologica Scandinavica* **58**, 292–305.

CRONE, C. & LEVITT, D. G. (1984). Capillary permeability to small solutes. In *Handbook of Physiology*, section 2, *The Cardiovascular System*, vol. IV, part 1, *Microcirculation*, ed. RENKIN, E. M. & MICHEL, C. C., pp. 411–461. American Physiological Society, Bethesda, MD, USA.

CURRY, F. E. (1986). Determinants of capillary permeability: a review of mechanisms based on single capillary studies in the frog. *Circulation Research* **59**, 367–380.

CURRY, F. E. & MICHEL, C. C. (1980). A fibre matrix theory of capillary permeability. *Microvascular Research* **20**, 96–99.

EATON, B. M., LEACH, L. & FIRTH, J. A. (1992). Fetal capillary permeability in the isolated dually perfused lobule of term human placenta. *International Journal of Microcirculation: Clinical and Experimental* **11**, 452.

EATON, B. M., YUDILEVICH, D. L., BRADBURY, M. W. B. & BAILEY, D. J. (1977). Studies on capillary permeability and carriers at the foetal surface of the syncytiotrophoblast in the perfused guinea-pig placenta. *Biorheology* **14**, 206.

FRAKER, P. J. & SPECK, J. C. (1978). Protein and cell membrane iodinations with a sparingly soluble chloramide, 1,3,4,6-tetrachloro-3a,6a diphenylglycouril. *Biochemical and Biophysical Research Communications* **80**, 849–857.

HARALDSSON, B. & RIPPE, B. (1985). Serum factors other than albumin are needed for the maintenance of normal capillary permselectivity in rat skeletal muscle. *Acta Physiologica Scandinavica* **129**, 127–135.

HEINRICH, D., METZ, E., RAVIOLA, E. & FORSSMANN, W. G. (1976). Ultrastructure of perfusion-fixed fetal capillaries in the human placenta. *Cell and Tissue Research* **172**, 157–169.

LEACH, L. & FIRTH, J. A. (1992). Fine structure of the paracellular junctions of terminal villous capillaries in the perfused human placenta. *Cell and Tissue Research* **268**, 447–452.

LEVICK, J. R. & MICHEL, C. C. (1973). The effect of bovine albumin on the permeabilities of frog mesenteric capillaries. *Quarterly Journal of Experimental Physiology* **58**, 87–97.

MANN, G. E. (1981). Alterations of myocardial capillary permeability by albumins in the isolated, perfused rabbit heart. *Journal of Physiology* **319**, 311–323.

MANN, G. E., SMAJE, L. H. & YUDILEVICH, D. L. (1979). Permeability of the fenestrated capillaries in the cat submandibular gland to lipid-insoluble molecules. *Journal of Physiology* **297**, 335–354.

MARTÍN DE JULÍAN, P. & YUDILEVICH, D. L. (1964). A theory for the quantification of transcapillary exchange by tracer dilution curves. *American Journal of Physiology* **207**, 162–168.

MASON, J. C., CURRY, F. E. & MICHEL, C. C. (1977). The effects of proteins upon the filtration coefficient of individually perfused frog mesenteric capillaries. *Microvascular Research* **13**, 185–202.

MICHEL, C. C. (1988). Capillary permeability and how it may change. *Journal of Physiology* **404**, 1–29.

MONTESANO, R., MOSSAZ, A., RYSER, J.-E., ORCI, L. & VASSALLI, P. (1984). Leukocyte interleukins induce cultured endothelial cells to produce a highly organised, glycosaminoglycan-rich pericellular matrix. *Journal of Cell Biology* **99**, 1706–1715.

PAASKE, W. P. (1977). Capillary permeability in skeletal muscle. *Acta Physiologica Scandinavica* **101**, 1–14.

PAASKE, W. P. & SEJRSEN, P. (1989). Permeability of continuous capillaries. *Danish Medical Bulletin* **36**, 570–590.

PAPPENHEIMER, J. R., RENKIN, E. M. & BORRERO, L. M. (1951). Filtration, diffusion and molecular seiving through peripheral capillary membranes. A contribution to the pore theory of capillary permeability. *American Journal of Physiology* **167**, 13–46.

RENKIN, E. M. (1959). Transport of potassium-42 from blood to tissues in isolated mammalian skeletal muscles. *American Journal of Physiology* **197**, 1205–1210.

REVIRIEGO, J., ALONSON, M. J., IBAÑEZ, C. & MARÍN, J. (1990). Action of adenosine and characterization of adenosine receptors in human placental vasculature. *General Pharmacology* **21**, 227–233.

SCHNEEBERGER, E. E. & HAMELIN, M. (1984). Interaction of serum proteins with lung endothelial glycocalyx: its effect on endothelial permeability. *American Journal of Physiology* **247**, H206–217.

SIBLEY, C. P., BAUMAN, K. F. & FIRTH, J. A. (1982). Permeability of the foetal capillary endothelium of the guinea-pig placenta to haem proteins of various molecular sizes. *Cell and Tissue Research* **223**, 165–178.

SIMIONESCU, N., SIMIONESCU, M. & PALADE, G. (1973). Permeability of muscle capillaries to exogenous myoglobin. *Journal of Cell Biology* **57**, 424–452.

SWEIRY, J. H. & MANN, G. E. (1991). Pancreatic microvascular permeability in caerulein-induced acute pancreatitis. *American Journal of Physiology* **261**, G685–692.

THORNBURG, K. L. & FABER, J. J. (1976). The steady state concentration gradients of an electron-dense marker (ferritin) in the three-layered hemochorial placenta of the rabbit. *Journal of Clinical Investigation* **58**, 912–925.

TRAP-JENSEN, J. & LASSEN, N. A. (1970). Capillary permeability for small hydrophobic tracers in exercising skeletal muscle in normal man and patients with long-term diabetes mellitus. In *Alfred Benzon Symposium II*, ed. CRONE, C. & LASSEN, N. A., pp. 135–152. Munksgaard, Copenhagen.

WARD, B. J., BAUMAN, K. F. & FIRTH, J. A. (1988). Interendothelial junctions of cardiac capillaries in rats: their structure and permeability properties. *Cell and Tissue Research* **252**, 57–66.

WHEELER, C. P. D. & YUDILEVICH, D. L. (1988). Transport and metabolism of adenosine in the perfused guinea-pig placenta. *Journal of Physiology* **405**, 511–526.

YUDILEVICH, D. L. & DE ROSA, N. (1971). Blood–brain transfer of glucose and other molecules measured by rapid indicator dilution. *American Journal of Physiology* **220**, 841–846.